Z. angew. Math. Phys. 52 (2001) 680–695
0010-2571/01/040680-16 $ 1.50+0.20/0

Zeitschrift für angewandte Mathematik und Physik ZAMP

Effects of inclusions in ductile cracks

B. M. Singh, H. T. Danyluk, A. P. S. Selvadurai, R. S. Dhaliwal, J. Rokne and J. Vrbik

Abstract. This paper examines the problems of the symmetric indentation of a ductile penny-shaped crack by an embedded rigid, thin, circular disc inclusion and a ductile Griffith crack by a line inclusion. The Dugdale hypothesis is adopted to determine the length of the plastic zone. Expressions for the resultant pressures applied to the inclusions are obtained. Numerical results for the length of plastic zones and resultant pressures are obtained and are displayed graphically.

Keywords. Ductile penny-shaped crack, ductile Griffith crack, triple integral equation, Fredholm integral equation of the second kind, plastic zone, stress intensity factor, fracture mechanics, inclusions in elastic media.

1. Introduction

The inclusion represents approximately a foundation which is deeply embedded in a material. The category of two and three-dimensional problems which deal with inclusions is of interest in the study of composite materials. Detailed accounts of inclusion problems in classical elasticity are given by Selvadurai and Singh[1] and Mura[2]. Stress analysis of the interaction between cracks and inclusions is of particular interest in the study of thermally and environmentally induced degradation of multiphase composites. The Dugdale model of a crack in a ductile material was introduced to investigate the extent of the inelastic zone at the ends of a stationary slit in a steel sheet under tension. The Dugdale model predictions agree closely with experimental results [3]. Uniform internal stresses equal to the material yield stress are prescribed in the inelastic regions so that the stress singularities at the crack tips do not appear.

An important study of the Dugdale model is also done by Rice[4]. To see this, the Dugdale hypothesis should be considered a working tool, rather than a precise description of the behavior of ductile material at the crack tip.

It is important to mention the results of the Dugdale penny-shaped crack discussed by Keer and Mura[5]. Selvadurai and Singh[6, 7] have examined the problem of the internal indentation of a penny-shaped inclusion of finite thickness in an isotropic elastic solid. In the case of a solid disc-shaped inclusion, the solution to

a particular problem can be obtained as a limiting case of the relevant problem for an oblate spheroidal inclusion. The spheroidal inclusion problem can be examined by making use of the direct spheroidal harmonic function technique discussed by Selvadurai[8].

In this paper two problems *Problem A*, a 3D problem, and *Problem B*, a 2D problem, are considered. To distinguish the problems the 3D problem is called *Problem A* and the 2D problem *Problem B*. In both problems, the inclusions and matrices have the same elastic moduli. Problem (A), in 3D, considers the indentation of a penny-shaped crack by a smooth rigid disc in an elastic material and the singularity in the normal stress present at the leading edge which arise using elastic theory is removed by adopting the Dugdale hypothesis. Therefore, this mixed boundary value problem is reduced to the solution of triple integral equations involving Bessel functions and then finally to a Fredholm integral equation of the second kind. On solving the Fredholm integral equation, numerical results for the length of the plastic-zone and the axial stiffness of the inclusion are obtained and shown graphically. As in the case for a brittle solid, if the plastic domain surrounding the penny-shaped inclusion is diminished then the crack tends to become penny-shaped. In other words, problem (A) is an extension of the work discussed by Selvadurai and Singh[6, 7].

Problem (B), in 2D, considers a two-dimensional problem of an elastic material and examines the effect of a rigid line inclusion with thickness on a ductile Griffith crack. Dugdale's hypothesis is again adopted to reduce the solution to triple integral equations involving cosine functions. A closed form solution of the triple integral equations is obtained and results for the length of the plastic zone and the resultant pressure on the inclusion are shown graphically. However, in Problem (B), Dugdale's slit-like crack does not tend to a penny-shaped crack. More explanations of Problems (A) and (B) are given in Sections 2 and 4 of this paper.

The class of problems relating to the behavior of flexible or rigid disc-shaped inclusions embedded in an elastic medium is of interest in geomechanics and studies of multiphase elastic materials. In geomechanical applications, the rigid disc-shaped inclusion represents the behavior of an earth or rock anchor which is created by the hydraulic fracture of the earth or rock mass. The disc-shaped region represents the resinous or cementing material which is used to transfer the anchoring loads to the geologic medium. The hypothesis of rigid inclusion is more solid in the context of composite materials when soils are too plastic to fit the hypotheses. Rock seems to be the more appropriate case, but the injection techniques related to anchor technology are so crude that a disc geometry may be far from reality.

Major applications of this paper lie in the area of strengthening engineering structures through the use of composite materials employing rigid inclusions by determining the strength and safety of the materials against both ductile and brittle fracture. The results of this paper can be used for quasi-brittle solids or metals. This is of importance in the area of materials science and an application

to some specific materials is presented.

The three-dimensional problem (a)

2. Boundary conditions, fundamental equations and integral equations

The indentation of a penny-shaped crack in an elastic material with $r \in (0, \infty)$, $z \in (-\infty, \infty)$ by a smoothly embedded rigid penny-shaped inclusion of thickness 2Δ is considered. Since the problem exhibits a state of symmetry about the plane $z = 0$, we can restrict our attention to a single half-space region occupying $z \geq 0$. The displacement and stress fields should reduce to zero as $(r^2 + z^2)^{\frac{1}{2}} \to \infty$. We are considering axially-symmetric deformation of the material under the Dugdale assumption which is that there is a thin annular region of inelastic deformation surrounding the penny-shaped crack. The inelastic zone is described by an inner radius b and an outer radius c. A tensile stress Y is uniformly distributed in the region. Boundary conditions on the plane $z = 0$ are

$$\sigma_{rz}(r,0) = 0, \quad r \geq 0 \tag{1}$$

$$u_z(r,0) = 0, \quad c \leq r < \infty \tag{2}$$

$$u_z(r,0) = \Delta, \quad 0 < r \leq a \tag{3}$$

$$\sigma_{zz}(r,0) = \begin{cases} 0, & a < r < b \\ Y, & b < r < c. \end{cases} \tag{4}$$

The formulation of Problem (A) is shown in Figure 1. In the plastic region the non-zero stress components σ_{rr}, $\sigma_{\theta\theta}$, σ_{zz} and σ_{rz} must satisfy a yield criterion. Because of the assumed nature of the plastic zone, the normal stress σ_{zz} does not vary too greatly over the zone. So σ_{zz} is set equal to the constant yield stress Y. To satisfy the von Mises yield criterion, the stresses σ_{rr}, $\sigma_{\theta\theta}$ and σ_{zz} are equated to zero. u_r and u_z are displacement components.

The solution of the equilibrium equation in terms of an unknown function $\mathrm{A}(s)$, which automatically frees the plane $z = 0$ from shear stress σ_{rz} is:

$$\left.\begin{aligned} u_r(r,z) &= \int_0^\infty [zs - (1-2\nu)]\mathrm{A}(s)\mathrm{J}_1(rs)e^{-sz}ds \\ u_z(r,z) &= \int_0^\infty [2(1-\nu) + sz)]\mathrm{A}(s)\mathrm{J}_0(rs)e^{-sz}ds \end{aligned}\right\}. \tag{5}$$

The corresponding normal stress is

$$\sigma_{zz} = -2\mathrm{G}\int_0^\infty [zs^2 + s]e^{-sz}\mathrm{A}(s)\mathrm{J}_0(rs)ds, \tag{6}$$

where $\mathrm{J}_{q_1}()$ is the Bessel function of the first kind of order $q_1 \geq 0$. G and ν are the shear modulus and Poisson's ratio respectively.

With minor change of notation equations (5) and (6) may be obtained from Sih([10], p. 53). The boundary conditions (2) to (4) yield the following triple

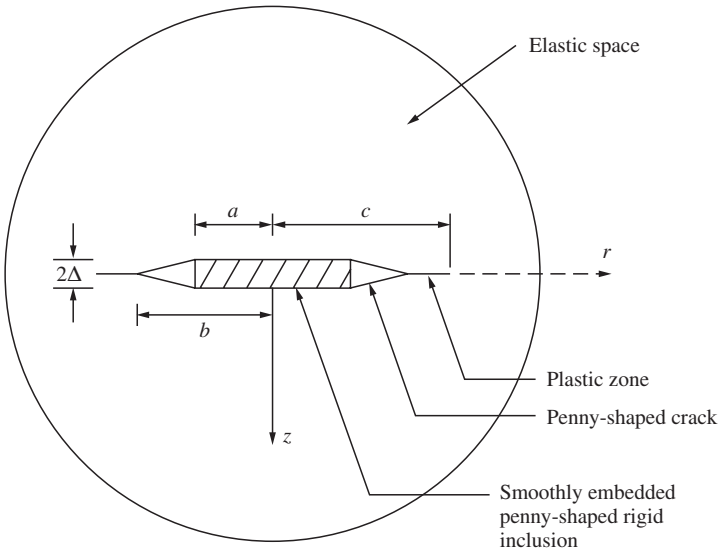

Figure 1. Penny-shaped rigid inclusion in smooth contact in a ductile penny-shaped crack.

integral equations:

$$\int_0^\infty \mathrm{A}(s)\mathrm{J}_0(rs)ds = \frac{\Delta}{2(1-\nu)}, \quad 0 < r < a, \tag{7}$$

$$\int_0^\infty s\mathrm{A}(s)\mathrm{J}_0(rs)ds = p(r), \quad a < r < c, \tag{8}$$

$$\int_0^\infty \mathrm{A}(s)\mathrm{J}_0(rs)ds = 0, \quad c < r < \infty, \tag{9}$$

where

$$p(r) = \left\{ \begin{array}{ll} 0 & a < r < b \\ -\frac{Y}{2\mathrm{G}} & b < r < c \end{array} \right\}. \tag{10}$$

3. Solution of the three-dimensional problem (A)

To obtain the solution of the triple integral equations (7), (8) and (9) let us set

$$\int_0^\infty s\mathrm{A}(s)\mathrm{J}_0(s)ds = \left\{ \begin{array}{ll} N_1(r) & 0 < r < a \\ N_3(r) & c < r < \infty. \end{array} \right\} \tag{11}$$

Making use of the Hankel transform, we obtain from equations (8), $(11)_1$ and $(11)_2$ that

$$\mathrm{A}(s) = \left[\int_0^a rN_1(r)\mathrm{J}_0(rs)dr + \int_a^c rp(r)\mathrm{J}_0(rs)dr + \int_c^\infty rN_3(r)\mathrm{J}_0(rs)dr \right]. \tag{12}$$

If we substitute equation (12) into equations (7) and (9), we find that

$$\mathrm{I}_1(r)+\mathrm{I}_2(r)+\mathrm{I}_3(r) = \frac{\Delta}{2(1-\nu)},\ \ 0<r<a, \tag{13}$$

$$\mathrm{I}_1(r)+\mathrm{I}_2(r)+\mathrm{I}_3(r) = 0,\ \ c<r<\infty, \tag{14}$$

where

$$\mathrm{I}_j=\int \lambda N_j(\lambda)\mathrm{L}(r,\lambda)d\lambda,\ \ (j=1,2,3; N_2(\lambda)=p(\lambda)), \tag{15}$$

the limits being 0 to a, a to c and c to ∞, respectively, and

$$\mathrm{L}(r,\lambda)=\int_0^\infty \mathrm{J}_0(ru)\mathrm{J}_0(\lambda u)du. \tag{16}$$

Making use of the paper by Selvadurai and Singh[9] equations (13) and (14) can be written in the following form:

$$\mathrm{E}_1(r)+\frac{2}{\pi}\int_c^\infty \frac{s\mathrm{E}_3(s)ds}{s^2-r^2} = \mathrm{G}_1(r),\ \ 0<r<a, \tag{17}$$

$$\mathrm{E}_3(r)+\frac{2}{\pi}r\int_0^a \frac{\mathrm{E}_1(s)ds}{r^2-s^2} = \mathrm{G}_2(r),\ \ c<r<\infty,, \tag{18}$$

where

$$\mathrm{G}_1(r) = \frac{\Delta}{2(1-\nu)}+\frac{Y}{2\mathrm{G}}[\sqrt{c^2-r^2}-\sqrt{b^2-r^2}],\ \ 0<r<a, \tag{19}$$

$$\mathrm{G}_2(r) = -\frac{Y}{2\mathrm{G}}[\sqrt{r^2-c^2}-\sqrt{r^2-b^2}],\ \ c<r<\infty, \tag{20}$$

$$\mathrm{E}_1(s) = \int_s^a \frac{\lambda N_1(\lambda)d\lambda}{(\lambda^2-s^2)^{\frac{1}{2}}},\ \ 0<s<a, \tag{21}$$

$$\mathrm{E}_3(s) = \int_c^s \frac{\lambda N_3(\lambda)d\lambda}{(s^2-\lambda^2)^{\frac{1}{2}}},\ \ c<s<\infty. \tag{22}$$

Equations (21) and (22) are also of Abel type integral equations and their solutions can be written as:

$$N_1(r) = -\frac{2}{\pi r}\frac{d}{dr}\int_r^a \frac{u\mathrm{E}_1(u)du}{(u^2-r^2)^{\frac{1}{2}}},\ \ 0<r<a, \tag{23}$$

$$N_3(r) = \frac{2}{\pi r}\frac{d}{dr}\int_c^r \frac{u\mathrm{E}_3(u)du}{(r^2-u^2)^{\frac{1}{2}}},\ \ c<r<\infty. \tag{24}$$

Using equations (6), (11) and (23), we find that

$$\sigma_{zz}(r,0)=\frac{4}{\pi r}\frac{d}{dr}\int_r^a \frac{u\mathrm{E}_1(u)du}{(u^2-r^2)^{\frac{1}{2}}}\ \ 0<r<a, \tag{25}$$

and that the resultant pressure on the inclusion is

$$\mathrm{P}=-2\pi\int_0^a r\sigma_{zz}(r,0)dr. \tag{26}$$

Using equation (25), we find from equation (26) that

$$\mathrm{P} = 8\mathrm{G}\int_0^a \mathrm{E}_1(u)du. \tag{27}$$

We readily find on using equations (6), (11) and (24) that

$$\sigma_{zz}(r,0) = -\frac{4\mathrm{G}}{\pi}\left[\frac{\mathrm{E}_3(c)}{(r^2-c^2)^{\frac{1}{2}}} + \int_c^r \frac{\mathrm{E}_3'(u)du}{(r^2-u^2)^{\frac{1}{2}}}\right], \quad c < r < \infty, \tag{28}$$

where the prime operator denotes the differentiation with respect to u. With the help of the Dugdale model, the stress intensity factor is zero at $r = c$. Therefore, we find that

$$\mathrm{K}_{\mathrm{I}}^c = \lim_{r\to c^+}[\sqrt{(r-c)}\sigma_{zz}(r,0)] = 0 \tag{29}$$

or on using equation (28) we obtain

$$\mathrm{K}_{\mathrm{I}}^c = \mathrm{E}_3(c) = 0. \tag{30}$$

Let $r = ar_1$, $s = cs_1$ and

$$\left.\begin{array}{rcl} \frac{\Delta \mathrm{F}_1(r)}{2(1-\nu)} & = & \mathrm{E}_1(ar_1) \\ \frac{\Delta}{2(1-\nu)}\mathrm{F}_2(r) & = & \mathrm{E}_3(cr_1). \end{array}\right\} \tag{31}$$

Using equations (19), (20) and (31), equations (17) and (18) can be written in the following form:

$$\mathrm{F}_1(r_1) + \frac{2}{\pi}\int_1^\infty \frac{s_1\mathrm{F}_2(s_1)ds_1}{(s_2^2 - \frac{a^2r_1^2}{c^2})} = 1 + \frac{Ya(1-\nu)}{\mathrm{G}\Delta}\left[\sqrt{\frac{c^2}{a^2}-r_1^2} - \sqrt{\frac{b^2}{a^2}-r_1^2}\right], \quad 0 < r_1 < 1 \tag{32}$$

$$\mathrm{F}_2(r_1) + \frac{2cr_1}{a\pi}\int_0^1 \frac{\mathrm{F}_1(s_1)ds_1}{(\frac{c^2r_1^2}{a^2} - s_1^2)} = -\frac{cY(1-\nu)}{\mathrm{G}\Delta}\left[\sqrt{r_1^2-1} - \sqrt{r_1^2-\frac{b^2}{c^2}}\right], \quad 1 < r_1. \tag{33}$$

Making use of equations (31), equations (27) and (30) can be written in the form:

$$\frac{(1-\nu)\mathrm{P}}{4\mathrm{G}\Delta a} = \int_0^1 \mathrm{F}_1(r_1)dr_1, \tag{34}$$

$$\mathrm{K}_{\mathrm{I}}^c = \mathrm{F}_2(1) = 0. \tag{35}$$

For finding the limiting cases, as $\frac{b}{a}$ becomes large, and therefore $a \to 0$. Hence from equations (33), (34) and (35), we get

$$b = c, \text{ and} \tag{36}$$

$$\frac{(1-\nu)\mathrm{P}}{4\mathrm{G}\Delta a} = 1. \tag{37}$$

Substituting the value of $\mathrm{F}_2(r_1)$ from equation (33) into equation (32), we get the following Fredholm integral equation of the second kind, namely:

$$\mathrm{F}_1(\eta) + \int_0^1 \mathrm{F}_1(\xi)\mathrm{K}(\eta,\xi)d\xi = f(\eta), \quad 0 < \eta < 1, \tag{38}$$

with the kernel function

$$\mathrm{K}(\eta,\xi) = \begin{cases} -\frac{2}{\pi^2(\eta^2-\xi^2)}\left[n\log\mid\frac{\overline{c}+\eta}{\overline{c}-\eta}\mid -\xi\log\mid\frac{\overline{c}+\xi}{\overline{c}-\xi}\mid\right], (\eta\neq\xi), \\ -\frac{2}{\pi^2}\left[\frac{\overline{c}}{(\overline{c}^2-\eta^2)}+\frac{1}{2\eta}\log\mid\frac{\overline{c}+\eta}{\overline{c}-\eta}\mid\right], (\eta=\xi), \end{cases} \tag{39}$$

and the free term of the integral equation,

$$f(\eta) = 1 + \frac{2\Omega}{\pi}\left[(\overline{c}^2-\overline{b}^2)^{\frac{1}{2}} - (\overline{b}^2-\eta^2)^{\frac{1}{2}}\tan^{-1}\left(\frac{\overline{c}^2-\overline{b}^2}{\overline{b}^2-\eta^2}\right)^{\frac{1}{2}}\right]. \tag{40}$$

$$\text{where } \overline{b} = \frac{b}{a}, \overline{c} = \frac{c}{a}, \text{ and } \Omega = \frac{Y(1-\nu)}{\mathrm{G}\Delta/a}. \tag{41}$$

The condition (35) can be expressed with the help of equations (33) and (41) as

$$\epsilon = \frac{2\overline{c}}{\pi}\int_0^1 \frac{\mathrm{F}_1(\xi)d\xi}{(\overline{c}^2-\xi^2)} - \Omega(\overline{c}^2-\overline{b}^2)^{\frac{1}{2}}, \tag{42}$$

where ϵ is the error function.

To solve the integral equation (38) the interval $(0,1)$ is divided into N segments with $h = 1/N$ and $\eta_i = (i-1/2)$ with $i = 1,2,3,\ldots,$. Then equation (38) can be replaced by

$$\mathrm{A}_{ij}\mathrm{F}_1(\eta_j) \approx f(\eta_i), \tag{43}$$

where

$$\mathrm{A}_{ij} = \delta_{ij} + \mathrm{K}(\eta_i,\eta_j)h \tag{44}$$

and

$$\delta_{ij} = \begin{cases} 1, & i = j \\ 0, & i \neq j \end{cases} \tag{45}$$

and the condition (42) is

$$\epsilon = \frac{2\overline{c}h}{\pi}\sum_{i=1}^{N}\left[\frac{\mathrm{F}_1(\eta_i)}{(\overline{c}^2-\eta^2)}\right] - \Omega[\overline{c}^2-\overline{b}^2]^{\frac{1}{2}} = 0. \tag{46}$$

As $\overline{c}$ is an unknown of the problem, the solution of (43) requires an initial assumed value of $\overline{c}$ and so that the error function given by (46) approaches zero. The results for $\frac{l}{a}$ or $(\frac{c-b}{a})$ and $\frac{\mathrm{P}(1-\nu)}{4\mathrm{G}\Delta a}$ are illustrated in the accompanying figures 3-4.

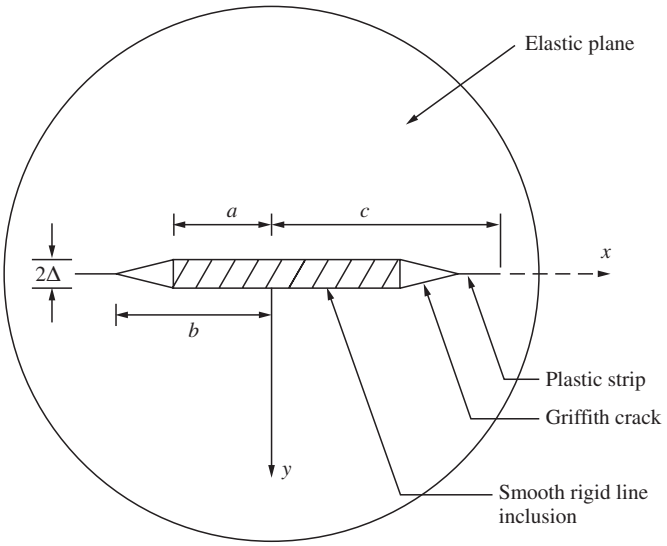

Figure 2. Line-shaped rigid inclusion in smooth contact in a ductile Griffith crack.

The two-dimensional problem (b)

4. Boundary conditions, fundamental equations and integral equations

In this section, we consider the two-dimensional counterpart to Problem (A) solved for a three-dimensional medium. Consider an elastic-plastic region $-\infty < x < \infty$, $-\infty < y < \infty$, which is bounded internally by a Griffith crack and is indented by a smooth rigid inclusion of thickness $2\overset{*}{h}$. Due to symmetry along the line $y = 0$, we restrict our attention to a single half-space region occupying $y \geq 0$. Boundary conditions can be written in the following form:

$$\sigma_{xy}(x,0) = 0, \quad x \geq 0, \tag{47}$$

$$u_y(x,0) = 0, \quad c < x < \infty, \tag{48}$$

$$u_y(x,0) = \overset{*}{h}, \quad 0 < x \leq a, \tag{49}$$

$$\sigma_{yy}(x,0) = \begin{cases} 0, & a < x < b \\ Y, & b < x < c. \end{cases} \tag{50}$$

Stresses and displacements should reduce to zero as $(x^2 + y^2)^{\frac{1}{2}} \to \infty$. The formulation of this problem is shown in Figure 2. The solution of the equilibrium equation in terms of an unknown function $\mathrm{B}_1(\alpha)$ is given by

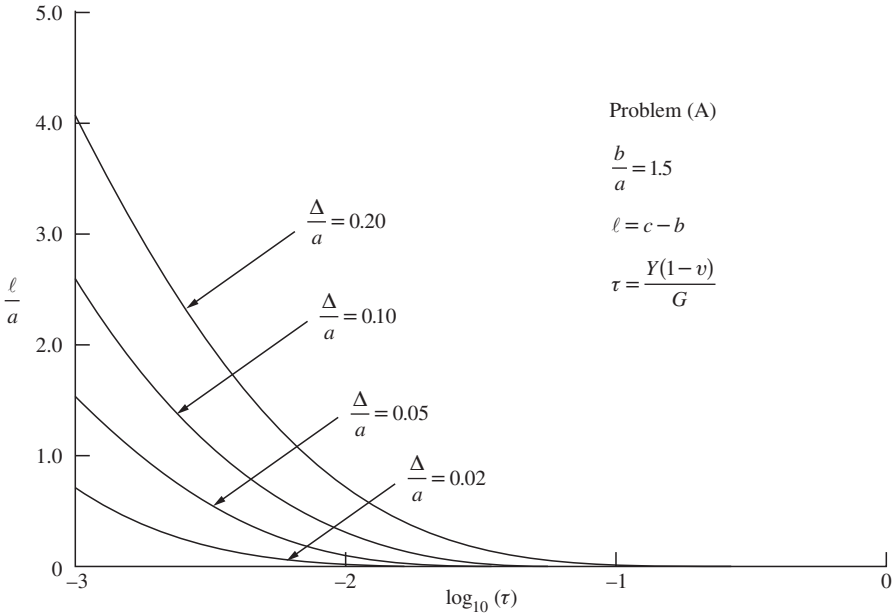

Figure 3. Variation of $\frac{l}{a}$ versus $\log_{10}(\tau)$ for different values of $\frac{\Delta}{a} = 0.20, 0.10, 0.05, 0.02$ with $\frac{b}{a} = 1.5$, $\tau = \frac{Y(1-\nu)}{\mathrm{G}}$, $l = c - b$.

$$\left.\begin{array}{rcl} u_x(x,y) & = & \frac{1+\nu}{\mathrm{E}} \int_0^\infty [(\alpha y - (1-2\nu)]\mathrm{B}_1(\alpha) e^{-\alpha y} \sin(\alpha x) d\alpha \\ u_y(x,y) & = & \frac{1+\nu}{\mathrm{E}} \int_0^\infty [2(1-\nu) + \alpha y]\mathrm{B}_1(\alpha) e^{-\alpha y} \cos(\alpha x) d\alpha \end{array}\right\} \tag{51}$$

The corresponding stress components are:

$$\sigma_{yy} = -\int_0^\infty \alpha(1+\alpha y)\mathrm{B}_1(\alpha) e^{-\alpha y} \cos(\alpha x) d\alpha, \tag{52}$$

$$\sigma_{xy} = -y \int_0^\infty \alpha^2 \mathrm{B}_1(\alpha) \sin(\alpha x) e^{-\alpha y} d\alpha, \tag{53}$$

where E and ν are Young's modulus and Poisson's ratio respectively. Making use of results from Sih([10], p. 136) equations (51)- (53) may be obtained for the case of plane strain.

The mixed boundary conditions (47)-(50) reduce the problem to the solution of the following integral equations:

$$\int_0^\infty \mathrm{B}_1(\alpha) \cos(\alpha x) d\alpha = \frac{\overset{*}{h}\,\mathrm{E}}{2(1-\nu^2)}, \quad 0 < x < a, \tag{54}$$

$$\int_0^\infty \alpha \mathrm{B}_1(\alpha) \cos(\alpha x) d\alpha = p_1(x), \quad a < x < c, \tag{55}$$

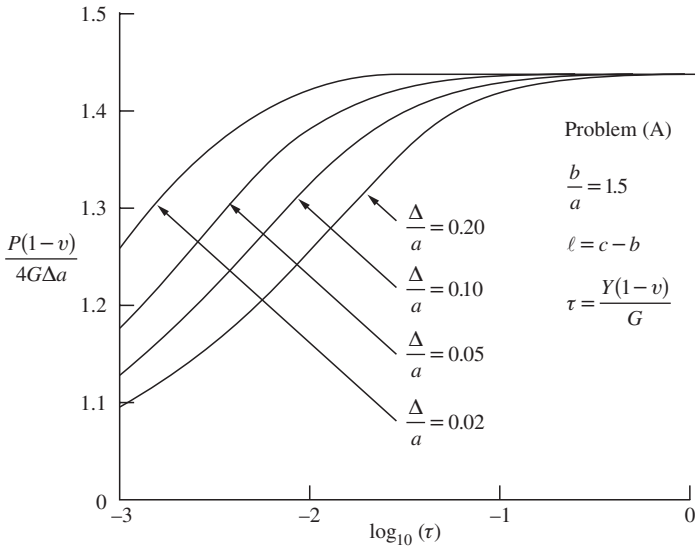

Figure 4. Variation of $\frac{\mathrm{P}(1-\nu)}{4\mathrm{G}\Delta a}$ versus $\log_{10}(\tau)$ for different values of $\frac{\Delta}{a}=0.20, 0.10, 0.05, 0.02$ with $\frac{b}{a}=1.5$, $\tau=\frac{Y(1-\nu)}{\mathrm{G}}$, $l=c-b$.

$$\int_0^\infty \mathrm{B}_1(\alpha)\cos(\alpha x)d\alpha \quad = \quad 0, \quad c<x<\infty, \tag{56}$$

where

$$p_1(x)=\begin{cases} 0, & a<x<b \\ -Y, & b<x<c. \end{cases} \tag{57}$$

5. Solution of the two-dimensional problem (B)

The solution of the triple integral equations (54), (55) and (56) can be written in the following form

$$\mathrm{B}_1(\alpha) \quad = \quad \frac{1}{\alpha}\int_a^c h(s)\sin(\alpha s)ds, \tag{58}$$

$$\begin{aligned} h(s) \quad &= \quad -\frac{4}{\pi^2}\left(\frac{s^2-a^2}{c^2-s^2}\right)^{\frac{1}{2}}\int_a^c\left(\frac{c^2-y^2}{y^2-a^2}\right)^{\frac{1}{2}}\frac{yp_1(y)dy}{y^2-s^2} \\ &+ \quad \frac{\mathrm{C}_1}{\sqrt{(c^2-s^2)(s^2-a^2)}}, \quad a<s<c, \end{aligned} \tag{59}$$

$$\mathrm{C}_1 \quad = \quad \frac{4c}{\pi^2\mathrm{F}}\int_a^c\left(\frac{s^2-a^2}{c^2-s^2}\right)^{\frac{1}{2}}ds\int_a^c\left(\frac{c^2-y^2}{y^2-a^2}\right)^{\frac{1}{2}}\frac{yp_1(y)dy}{y^2-s^2}$$

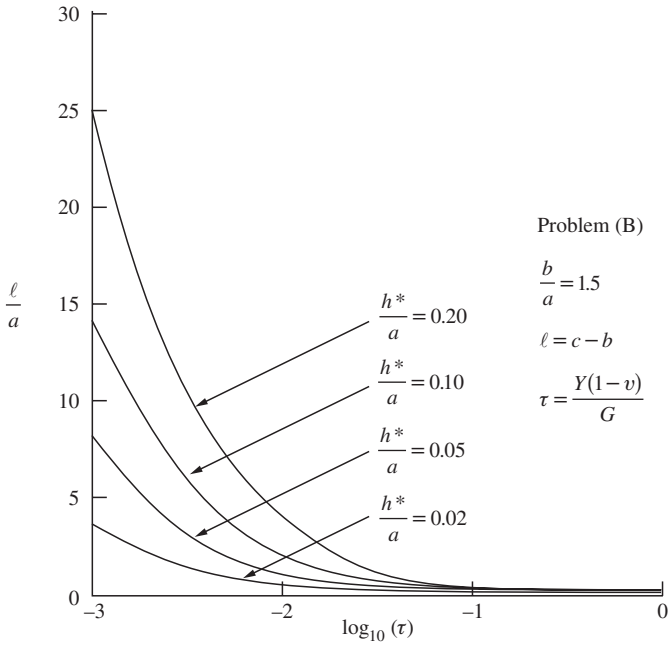

Figure 5. Variation of the length of the plastic zone $\frac{l}{a}$ versus $\log_{10}(\tau)$ for different values of $\frac{\overset{*}{h}}{a}=0.20,0.10,0.05,0.02$ with $\frac{b}{a}=1.5$, $\tau=\frac{Y(1-\nu)}{\mathrm{G}}$, $l=c-b$.

$$+ \quad \frac{c\,\overset{*}{h}\,\mathrm{E}}{\pi(1-\nu^2)\mathrm{F}}, \tag{60}$$

where F denotes the elliptic integral of the first kind with $\mathrm{F}=\mathrm{F}(\frac{\pi}{2},\sqrt{1-\frac{a^2}{c^2}})$.

Making use of equations (52), (58),(59) and (60), we get

$$[\sigma_{yy}(x,0)]_{x>c}=\frac{2}{\pi}\sqrt{\frac{x^2-a^2}{x^2-c^2}},$$
$$\int_a^c\left(\frac{c^2-y^2}{y^2-a^2}\right)^{\frac{1}{2}}\frac{yp_1(y)dy}{x^2-y^2}+\frac{\pi\mathrm{C}_1}{2\sqrt{(x^2-a^2)(x^2-c^2)}},\quad c<x. \tag{61}$$

We now find the stress intensity factor at $x=c$ in the form:

$$\begin{aligned}\mathrm{K}_c &= \lim_{x\to c^+}\sqrt{x-c}\sigma_{yy}(x,0)\\ &= \frac{2}{\pi\sqrt{2c(c^2-a^2)}}\left[(c^2-a^2)\int_a^c\frac{yp_1(y)dy}{[(y^2-a^2)(c^2-y^2)]^{\frac{1}{2}}}+\frac{\pi^2}{4}\mathrm{C}_1\right]\end{aligned} \tag{62}$$

With the Dugdale hypothesis in effect, we find that $\mathrm{K}_c=0$ at $x=c$. Making

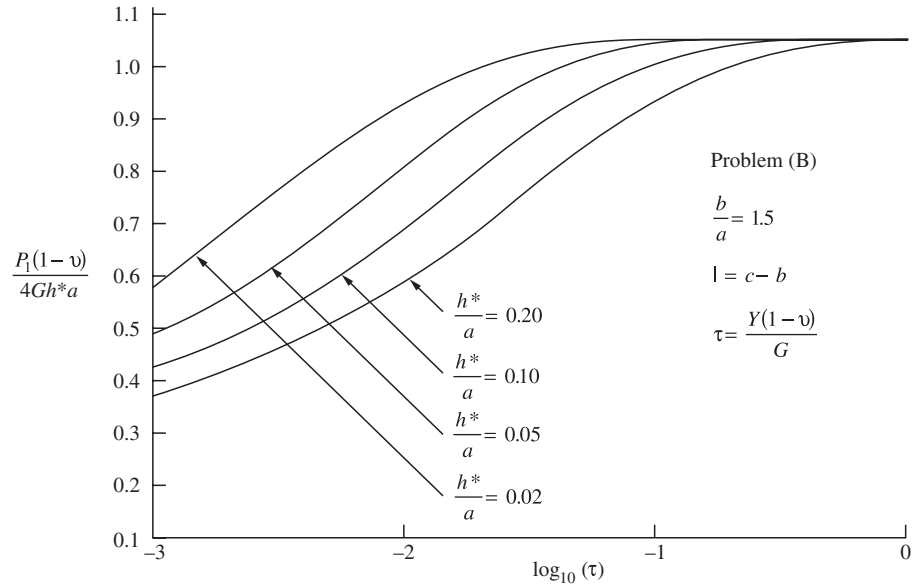

Figure 6. Variation of $\frac{\mathrm{P}_1(1-\nu)}{4\mathrm{G}\overset{*}{h}a}$ versus $\log_{10}(\tau)$ for different values of $\frac{\overset{*}{h}}{a} = 0.20, 0.10, 0.05, 0.02$ with $\frac{b}{a} = 1.5$, $\tau = \frac{Y(1-\nu)}{\mathrm{G}}$, $l = c - b$.

use of equations (57) and (62), we find that

$$\mathrm{C}_1 = \frac{2Y(c^2-a^2)}{\pi^2}\left[\frac{\pi}{2} + \sin^{-1}\left(\frac{a^2+c^2-2b^2}{c^2-a^2}\right)\right]. \tag{63}$$

In the same way, using (57) we get from equation (60) that

$$\begin{aligned}\mathrm{C}_1 &= \frac{2cY}{\pi^2\mathrm{F}}\int_a^c \left(\frac{s^2-a^2}{c^2-s^2}\right)^{\frac{1}{2}}\left[\frac{\pi}{2} + \sin^{-1}\left(\frac{a^2+c^2-2b^2}{c^2-a^2}\right)\right.\\ &+ \left.\left(\frac{c^2-s^2}{s^2-a^2}\right)^{\frac{1}{2}}\log\left|\frac{N(s)}{\mathrm{D}(s)}\right|\right]ds + \frac{c\overset{*}{h}\,\mathrm{E}}{\pi\mathrm{F}(1-\nu^2)},\end{aligned} \tag{64}$$

where

$$\begin{aligned}N(s) &= (c^2-a^2)(b^2-s^2)\\ \text{and}&\\ \mathrm{D}(s) &= 2(s^2-a^2)(c^2-s^2) + (b^2-s^2)(c^2+a^2-2s^2)\\ &+ 2[(c^2-s^2)(s^2-a^2)(-(b^2-s^2)^2\\ &+ (b^2-s^2)(c^2+a^2-2s^2) + (s^2-a^2)(c^2-s^2))]^{\frac{1}{2}}.\end{aligned} \tag{65}$$

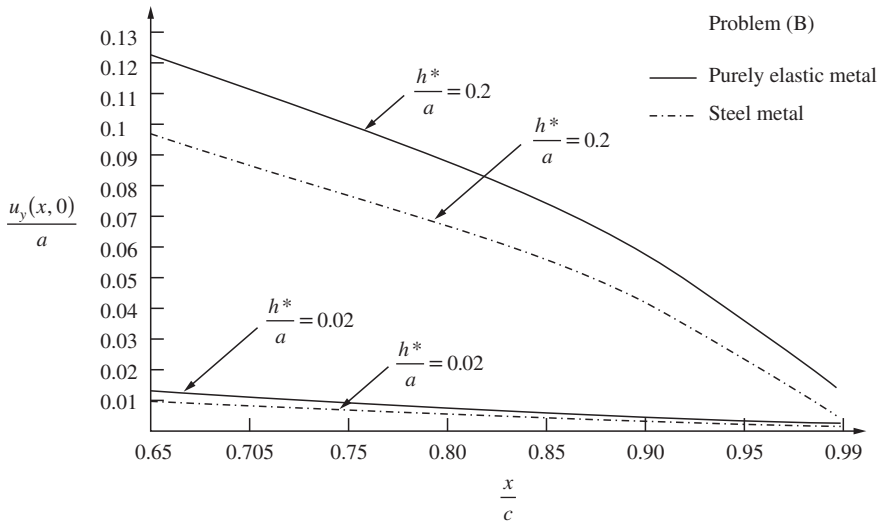

Figure 7. Comparison of the displacement component $\frac{u_y(x,0)}{a}$ for steel metal along the plastic strip with the desplacement component for purely elastic medium versus $\frac{x}{c}$ for different values of $\frac{\overset{*}{h}}{a} = .20, .02$ and $\frac{a}{c} = 0.4$, $\frac{b}{c} = 0.63$, $\nu = 0.30$.

Equations (63) and (64) now yield:

$$\frac{2}{\pi^2}(c^2-a^2)\Omega_1\left[\frac{\pi}{2}+\sin^{-1}\left(\frac{a^2+c^2-2b^2}{c^2-a^2}\right)\right] = \frac{c}{\pi \mathrm{F}} + \frac{2c\Omega_1}{\pi^2 \mathrm{F}}\int_a^c \left(\frac{s^2-a^2}{c^2-s^2}\right)^{\frac{1}{2}} \left[\frac{\pi}{2}+\sin^{-1}\left(\frac{a^2+c^2-2b^2}{c^2-a^2}\right)+\left(\frac{c^2-s^2}{s^2-a^2}\right)^{\frac{1}{2}}\log\mid\frac{N(s)}{\mathrm{D}(s)}\mid\right] ds \tag{66}$$

where

$$\Omega_1 = \frac{(1-\nu^2)Y}{\mathrm{E}\overset{*}{h}}. \tag{67}$$

The resultant pressure on the inclusion is:

$$\mathrm{P}_1 = -\int_0^a \sigma_{yy}(x,0)dx \tag{68}$$

and we find after some manipulation that

$$\begin{aligned}\mathrm{P}_1 &= \frac{Y}{\pi}\left[\int_0^a\left(\frac{\pi}{2}+\sin^{-1}\left(\frac{a^2+c^2-2b^2}{c^2-a^2}\right)\right)\left(\frac{c^2-x^2}{a^2-x^2}\right)^{\frac{1}{2}}dx\right] \\ &- \frac{Y}{\pi}\int_0^a\left[\frac{\pi}{2}-\tan^{-1}\left[\frac{-2(c^2-x^2)(x^2-a^2)+(b^2-x^2)(a^2+c^2-2x^2)}{\mathrm{D}^*(x)}\right]\right]dx \\ &+ \frac{\pi \mathrm{C}_2}{2c}\mathrm{F}_1,\end{aligned} \tag{69}$$

where

$$\begin{aligned} \mathrm{D}^*(x) &= 2[(c^2-x^2)(a^2-x^2)\{-(b^2-x^2)^2+(b^2-x^2)(a^2+c^2-2x^2) \\ &- (c^2-x^2)(a^2-x^2)\}]^{\frac{1}{2}}, \qquad (70) \\ \mathrm{C}_2 &= \frac{2cY}{\pi^2\mathrm{F}}\int_a^c \left[\left(\frac{c^2-x^2}{x^2-a^2}\right)^{\frac{1}{2}}\left[-\frac{\pi}{2}-\sin^{-1}\left(\frac{a^2+c^2-2b^2}{c^2-a^2}\right)\right]\right. \\ &+ \left.\log\mid\frac{N(x)}{\mathrm{D}(x)}\mid\right]dx+\frac{c\overset{*}{h}\,\mathrm{E}}{\pi\mathrm{F}(1-\nu^2)}, \qquad (71) \\ \mathrm{F}_1 &= \mathrm{F}\left(\frac{\pi}{2},\frac{a}{c}\right). \qquad (72) \end{aligned}$$

An expression for P_1 can now be determined on substituting this expression for C_2 into equation (69). Using equations (66), (69) and (70) and solving them numerically, the values of c and P_1 for different values of the yield stress are obtained. The results for this problem are illustrated in the accompanying Figures 5-7.

Making use of equations $(51)_2$ and (58), we find that

$$u_y(x,0)=\frac{\pi(1-\nu^2)}{\mathrm{E}}\int_x^c h(s)ds,\ \ a<x<c. \qquad (73)$$

With the help of equations (57), (59) and (60) we find from equation (73) that

$$\begin{aligned} u_y(x,0) &= \frac{2(1-\nu^2)Y}{\pi\mathrm{E}}\left[-\left(c\mathrm{E}(\lambda,q)-\frac{a^2}{c}\mathrm{F}(\lambda,q)\right)\sin^{-1}\left(\frac{c^2-b^2}{c^2-a^2}\right)^{\frac{1}{2}}\right. \\ &+ \left.\frac{1}{2}\int_x^c\log\left|\frac{\mathrm{G}_1(s)}{\mathrm{G}_2(s)}\right|ds\right]+\mathrm{C}_3\mathrm{F}(\lambda,q),\ a<x<c, \qquad (74) \end{aligned}$$

where

$$\begin{aligned} \mathrm{C}_3 &= \frac{-2Y(1-\nu^2)}{\pi\mathrm{EF}}\left[-\sin^{-1}\left(\frac{c^2-b^2}{c^2-a^2}\right)^{\frac{1}{2}}\left(c\mathrm{E}(\frac{\pi}{2},q)-\frac{a^2}{c}\mathrm{F}\right)\right. \\ &+ \left.\frac{1}{2}\int_a^c\log\left|\frac{\mathrm{G}_1(s)}{\mathrm{G}_2(s)}\right|ds\right]+\frac{h^*}{\mathrm{F}}, \qquad (75) \\ \mathrm{G}_1(s) &= [\{\sqrt{(s^2-a^2)(b^2-a^2)}-\sqrt{(c^2-s^2)(c^2-b^2)}\} \\ &+ c^2-a^2][(c^2-s^2)^{\frac{1}{2}}+(c^2-b^2)^{\frac{1}{2}}], \qquad (76) \\ \mathrm{G}_2(s) &= [c^2-a^2+\{\sqrt{(s^2-a^2)(b^2-a^2)} \\ &+ \sqrt{(c^2-s^2)(c^2-b^2)}\}][(c^2-s^2)^{\frac{1}{2}}-(c^2-b^2)^{\frac{1}{2}}]. \qquad (77) \end{aligned}$$

$\mathrm{F}(\lambda,q)$ is an elliptic integral of the second kind, where

$$\lambda=\sin^{-1}\left(\frac{c^2-x^2}{c^2-a^2}\right)^{\frac{1}{2}}. \qquad (78)$$

The integrals in (74) and (75) are convergent and their numerical values can be obtained easily.

When the elastic medium is purely elastic, then $Y = 0$. In that case, we get by using (74) and (75) that

$$u_y(x,0) = \frac{h^* \mathrm{F}(\lambda, q)}{\mathrm{F}}. \tag{79}$$

If we compare displacement equations (74) and (79), we find that the results given by equation (74) are different for each metal. In other words, the displacement component depends on the material properties. The displacement component given by equation (79) does not depend on elastic constants and the results are discussed in Figure No. 7.

6. Conclusions

The results of this paper are illustrated by graphs contained in Figures 3-7. They are applicable for metals and we have considered the following metals: steel, copper, magnesium, zinc alloy and aluminum.

METAL	E (P_a)	Y (P_a)	Y/E	ν	$\log_{10}(\tau)$
Steel	200×10^3	200	10^{-3}	0.30	-2.7399
Magnesium	45×10^3	150	3.33×10^{-3}	0.35	-2.2332
Zinc alloy	97×10^3	140	0.669×10^{-3}	0.25	-2.9015
Copper	115×10^3	69	0.600×10^{-3}	0.30	-2.9617
Aluminum	69×10^3	28	0.406×10^{-3}	0.33	-3.1405

Here $\tau = \frac{Y(1-\nu)}{\mathrm{G}} = \frac{2(1-\nu^2)Y}{\mathrm{E}}$.

For problem (A), involving the steel metal, it is seen from Figure 3 that as $\frac{\Delta}{a}$ increases, the length of the plastic zone increases and from Figure 4 that the value of P decreases as $\frac{\Delta}{a}$ increases.

For problem (B) involving the steel, Figures 5 and 6 show that as $\frac{\overset{*}{h}}{a}$ increases, the length of the plastic zone increases as P_1 decreases.

In the same way, results in the form of graphs (Fig. 3 - Fig. 6) can be used for copper, magnesium and zinc and alloy metals. If these graphs are extended then the results can be used for aluminum. In Figure 7 for problem (B), the displacement component for steel metal is compared with the displacement component for a purely elastic material.

References

[1] A. P. S. Selvadurai and B. M. Singh, Some annular disc inclusion problems in elasticity. Int. J. *Solids Structures* **20** (1984), 129-139.
[2] T. Mura, *Micromechanics of Defects in Solids,* Sijthoff and Nordhoff, The Netherlands (1982).
[3] D. S. Dugdale, Yielding of steel sheets containing slits. *J. Mech. Phys. Solids* **8** (1960), 100-104.
[4] J. R. Rice, *Mechanics of Solids.* edited by H. G. Hopkins and M. J. Sewell, Pergamon Press, Oxford (1982).
[5] L. M. Keer and T. Mura, Stationary cracks and continuous distribution of dislocations. *Proc. Int. Conf. Fracture* **1** (1966), 99-115.
[6] A. P. S. Selvadurai and B. M. Singh, On the expansion of a penny-shaped crack by a rigid circular disc inclusion, *Int. J. Fracture* **25** (1984), 69-77.
[7] A. P. S. Selvadurai and B. M. Singh, The axial displacement of a disc inclusion embedded in a penny-shaped crack, *Z. angew. Math. Phys. (ZAMP)* **37** (1986), 64-77.
[8] A. P. S. Selvadurai, The load-deflexion characteristics of a deep rigid anchor in elastic medium. *Geotechnique* **26** (1976), 603-612.
[9] A. P. S. Selvadurai and B. M. Singh, The annular crack problem for an isotropic elastic solid. *Quart. J. Mech. and Applied Math* **38** (1985), 233-243.
[10] G. C. Sih, *Methods of Analysis and Solutions of Crack Problems.* Nordhoff International Publishing, Leyden (1973).

H. T. Danyluk
Department of Mechanical Engineering
University of Saskatchewan
Saskatoon, Saskatchewan
Canada S7N-5A9

A. P. S. Selvadurai
Department of Civil Engineering
and Applied Mechanics
MacDonald Engineering Building
McGill University
817 Sherbrooke Street West
Montreal, PQ
Canada H3A 2K6

R. S. Dhaliwal, B. M. Singh
Department of Mathematics and Statistics
The University of Calgary
Calgary, Alberta
Canada T2N-1N4

J. Vrbik
Department of Mathematics
Brock University
St. Catharines, Ontario
Canada L2S-3A1

J. Rokne
Department of Computer Science
The University of Calgary
Calgary, Alberta
Canada T2NIN4

(Received: July 9, 1999; revised: March 1, 2000)